Reconsidering the change in global biosphere productivity between the Last Glacial Maximum and present day from the triple oxygen isotopic composition of air trapped in ice cores

A. Landais, J. Lathiere, E. Barkan, B. Luz

Reconsidering the change in global biosphere productivity between the Last Glacial Maximum and present day from the triple oxygen isotopic composition of air trapped in ice cores

A. Landais,[1] J. Lathiere,[2] E. Barkan,[1] and B. Luz[1]

Received 9 April 2006; revised 10 December 2006; accepted 11 January 2007; published 30 March 2007.

[1] We present a global model to infer past biosphere productivity using the record of triple isotopic composition of atmospheric oxygen. Our model incorporates recent determinations of the mass-dependent relationships between $\delta^{17}O$ and $\delta^{18}O$ associated with leaf transpiration and various O_2 uptake processes. It also considers the spatial and seasonal variations of vegetation distribution, climatic conditions, and isotopic composition of meteoric water. On the basis of this model, we provide global estimates for the Last Glacial Maximum (LGM) and the present of (1) the triple isotopic composition of leaf water, (2) isotopic fractionation factors for terrestrial dark respiration in soils and in leaves as well as total terrestrial respiration, (3) relationships between $\delta^{17}O$ and $\delta^{18}O$ associated with terrestrial biological steady state, and (4) ^{17}O anomalies issued from both the terrestrial and oceanic biospheres. Using these data and the vegetation distribution simulated by the ORCHIDEE model, we estimated that the rate of global biological productivity during the LGM was 60–75% of the present rate. Our value for the LGM is at the lower end of previous estimates and suggests that the rise in biosphere productivity since the last glacial is larger than previously thought.

Citation: Landais, A., J. Lathiere, E. Barkan, and B. Luz (2007), Reconsidering the change in global biosphere productivity between the Last Glacial Maximum and present day from the triple oxygen isotopic composition of air trapped in ice cores, *Global Biogeochem. Cycles*, *21*, GB1025, doi:10.1029/2006GB002739.

1. Introduction

[2] Among the main processes that affect global climate changes are the interactions between the atmosphere and biosphere. Climatic conditions control biosphere production and, in turn, vegetation strongly influences climate through the emission and consumption of greenhouse gases and through the terrestrial albedo. The only way to understand these interactions is to depict the past climate changes and the related biosphere evolution. While many different proxies exist that allow for reconstruction of past climates, our knowledge about the past biosphere remains very sketchy.

[3] For the most part, past biosphere evolution is inferred from local studies of terrestrial and marine sediments. An important representative property of the past biosphere, which is extensively measured in the ocean, is paleoproductivity [e.g., *Kohfeld et al.*, 2005]. These studies, however, give information only on local variations in biosphere productivity, and much effort in data compilation is needed to infer the evolution of biosphere productivity at the global scale.

[4] The triple isotopic composition of atmospheric oxygen is an additional tracer that reflects global oxygen biosphere productivity [*Luz et al.*, 1999]. This is because oxygen in the lower atmosphere is exchanged with the terrestrial and oceanic biosphere through photosynthesis and respiration, and with the stratosphere through mixing of tropospheric and stratospheric air. While O_2 fluxes associated with biosphere productivity modify the isotopic composition of atmospheric oxygen through mass-dependent fractionation (change in $^{17}O/^{16}O$ is about 0.52 of the change in $^{18}O/^{16}O$), stratospheric oxygen is fractionated in a mass-independent way (change in $^{17}O/^{16}O$ roughly equals the change in $^{18}O/^{16}O$) through photochemical reactions with ozone [*Thiemens et al.*, 1991; *Bender et al.*, 1994; *Luz et al.*, 1999]. As a result, atmospheric O_2 becomes depleted in ^{17}O in comparison to O_2 affected by biology alone. The magnitude of this depletion depends on the relative proportions of the oxygen fluxes associated with biosphere productivity and with the stratosphere exchange. In turn, records of past changes in the triple isotope ratios enable one to infer variations in past biosphere productivity.

[5] One of the major climatic changes documented in numerous studies is the last deglaciation, and thus this presents a highly important challenge to determine the productivity over this period. *Luz et al.* [1999] and *Blunier et al.* [2002] measured the triple isotopic composition of O_2 in the past atmosphere from air trapped in ice cores. On the basis of these data, *Luz et al.* [1999] presented a rough mass

[1] Institute of Earth Sciences, Edmond Safra Campus, Hebrew University of Jerusalem, Jerusalem, Israel.
[2] Institute Pierre Simon LaPlace/Laboratoire des Sciences du Climat et l'Environnement, CNRS/CEA, Gif sur Yvette, France.

0886-6236/07/2006GB002739

balance of three oxygen isotopes in the biosphere, stratosphere and lower atmosphere and provided a first estimate of the ratio between the Last Glacial Maximum (LGM) and the present-day oxygen biosphere productivities as 90%. *Blunier et al.* [2002] refined the method and estimated LGM paleoproductivity as 76–83% of the present value.

[6] In their model, *Blunier et al.* [2002] took into account the influence of every process associated with oxygen production and consumption on the oxygen fractionation. In the absence of precise determinations of the mass-dependent relationships between $\delta^{17}O$ and $\delta^{18}O$ associated with these processes, they assumed that the same relationship applies to all the different processes. However, recently developed analytical capabilities for precise measurements of the triple isotopic composition of oxygen in O_2 and in H_2O [*Barkan and Luz*, 2003, 2005] have made it possible to show significant differences in the relationships between $\delta^{17}O$ and $\delta^{18}O$ for the different mass-dependent processes affecting atmospheric O_2 [*Angert et al.*, 2003a; *Helman et al.*, 2005; *Landais et al.*, 2006]. These differences influence the triple isotopic composition of O_2 and, as shown by *Angert et al.* [2003a], at least 15% of the changes in the triple isotopic composition of oxygen in the past atmosphere should be related to the variations in these relationships among different respiration mechanisms. Taking into account other processes involved in biosphere productivity, the influence on the triple isotopic composition of O_2 can be even greater.

[7] *Blunier et al.* [2002] also used for their calculation spatial and temporal averages for climatic conditions, land vegetation cover and isotopic composition of meteoric water during the different climatic periods. However, *Hoffmann et al.* [2004] showed that the spatial and seasonal variations of these parameters significantly affect the isotopic composition of atmospheric O_2 produced by the biosphere, and should be also considered in correct estimations of past biosphere productivity. Therefore the estimate of the LGM oxygen biosphere productivity obtained by *Blunier et al.* [2002] may not be adequate.

[8] In the present work we describe a complete three oxygen isotopes mass balance model for atmospheric oxygen that takes into account the recently determined mass-dependent relationships between $\delta^{17}O$ and $\delta^{18}O$ in the biosphere and in leaf water, as well as the spatial and seasonal variations of climatic conditions, land vegetation cover and isotopic composition of meteoric water. On the basis of this model we recalculated the ratio between the LGM and the present-day oxygen biosphere productivities.

2. The ^{17}O Anomaly – $^{17}\Delta$

[9] The ^{17}O enrichment (or anomaly), $^{17}\Delta$, is defined as [*Miller*, 2002; *Luz and Barkan*, 2005]

$$^{17}\Delta = \ln\left(\delta^{17}O + 1\right) - \lambda \times \ln\left(\delta^{18}O + 1\right), \quad (1)$$

where $\delta^*O = (^*R/^*R_{ref} - 1)$ (the factor 1000 is omitted but the δ^*O values are reported in ‰) and λ is the slope of a line of mass-dependent fractionation on a $\ln(\delta^{17}O + 1)$ versus $\ln(\delta^{18}O + 1)$ plot.

[10] As in previous studies [*Luz and Barkan*, 2000, 2005; *Angert et al.*, 2003a], we report the extent to which an O_2 sample is enriched in ^{17}O with respect to the present atmosphere (atm, PST). For the calculation of $^{17}\Delta$ we use the reference slope λ corresponding to ordinary respiration, the most widespread biological mass O_2 consumption mechanism. In the present study we assume that atmospheric oxygen is at steady state; that is, photosynthesis equals respiration. In this case, λ equals 0.516 [*Angert et al.*, 2003a; *Luz and Barkan*, 2005]. By definition, the anomaly of the present atmosphere ($^{17}\Delta_{atm,PST}$) equals 0.

3. Budget of the Triple Isotopic Composition of Atmospheric Oxygen

[11] The ^{17}O anomaly of oxygen in the atmosphere, $^{17}\Delta_{atm}$, results from an oxygen isotopic balance between two important global processes: mass-dependent biospheric O_2 production and mass-independent stratospheric photochemistry involving O_2, O_3 and CO_2 [*Luz et al.*, 1999],

$$F_{bio} \times \left(^{17}\Delta_{bio} - {}^{17}\Delta_{atm}\right) = F_{strat} \times \left(^{17}\Delta_{strat} - {}^{17}\Delta_{atm}\right), \quad (2)$$

where $^{17}\Delta_{strat}$ and $^{17}\Delta_{bio}$ are the ^{17}O anomalies of the stratospheric O_2 flux (F_{strat}) and the biospheric O_2 flux (F_{bio}), respectively.

[12] The ratio of the oxygen biosphere productivity between the LGM and the present is calculated from equation (2) as

$$\frac{F_{bio,LGM}}{F_{bio,PST}} = \frac{F_{strat,LGM} \times \left(^{17}\Delta_{strat,LGM} - {}^{17}\Delta_{atm,LGM}\right)}{F_{strat,PST} \times \left(^{17}\Delta_{strat,PST} - {}^{17}\Delta_{atm,PST}\right)} \times \frac{\left(^{17}\Delta_{bio,PST} - {}^{17}\Delta_{atm,PST}\right)}{\left(^{17}\Delta_{bio,LGM} - {}^{17}\Delta_{atm,LGM}\right)}, \quad (3)$$

where subscripts bio, strat, atm, PST and LGM stand for total biosphere, stratosphere, lower atmosphere, present day and LGM, respectively. By definition (section 2) $^{17}\Delta_{atm,PST} = 0$, whereas $^{17}\Delta_{atm,LGM}$ was determined by *Blunier et al.* [2002] as +43 permeg (note that the original value of Blunier et al. is +38 permeg since it was calculated with λ of 0.521, instead of 0.516 accepted in the present study as a reference slope). Following *Luz et al.* [1999], we assumed that the ratio of the production rates of anomalously depleted O_2 in the stratosphere, $F_{strat} \times (^{17}\Delta_{strat} - {}^{17}\Delta_{atm})$, between the LGM and the present is proportional to the ratio of atmospheric CO_2 concentrations between the LGM and the pre-industrial Holocene. Then, using CO_2 concentrations of 280 ppmv for the pre-industrial Holocene and 190 ppmv for the LGM [*Barnola et al.*, 1987], equation (3) becomes

$$\frac{F_{bio,LGM}}{F_{bio,PST}} = \frac{190}{280} \times \frac{^{17}\Delta_{bio,PST}}{\left(^{17}\Delta_{bio,LGM} - 43\right)}. \quad (4)$$

[13] The quantification of past biosphere productivity from the triple isotopic composition of oxygen in the atmosphere is therefore highly dependent on the change in atmospheric concentration of CO_2 and on the precise

knowledge of the triple isotopic composition of oxygen produced by the biosphere, $^{17}\Delta_{bio}$, for the present and the LGM. Both ocean and land biospheres contribute to the global oxygen productivity so that $^{17}\Delta_{bio}$ is the weighted average of $^{17}\Delta$ issued from the oceanic biosphere, $^{17}\Delta_{ocean}$, and the terrestrial biosphere, $^{17}\Delta_{terr}$,

$$^{17}\Delta_{bio} = \frac{F_O \times {}^{17}\Delta_{ocean} + F_T \times {}^{17}\Delta_{terr}}{F_O + F_T} = \frac{(F_O/F_T) \times {}^{17}\Delta_{ocean} + {}^{17}\Delta_{terr}}{(F_O/F_T) + 1}, \quad (5)$$

where F_O and F_T are the oxygen fluxes associated with the oceanic and terrestrial productivities.

[14] For present-day conditions the different ocean and land biosphere models give an F_O/F_T ratio in the range of 0.45 to 0.59 [*Bender et al.*, 1994; *Blunier et al.*, 2002; *Hoffmann et al.*, 2004]. A global value for $^{17}\Delta_{ocean}$ was determined by *Luz and Barkan* [2000] as 249 ± 15 permeg, but no global estimate of $^{17}\Delta_{terr}$ is available. Likewise, there is no estimate of $^{17}\Delta_{ocean}$ and $^{17}\Delta_{terr}$ for the LGM.

4. Estimate of $^{17}\Delta_{ocean}$

[15] In order to estimate $^{17}\Delta_{ocean}$ for the LGM, we assumed that the fractionation during O_2 uptake was the same during the LGM and the present. Therefore any change in $^{17}\Delta_{ocean}$ between the LGM and the present is only due to the shift in the isotopic composition of the global ocean. The decrease of the ice sheet volume between the LGM and the present induced a decrease of 1‰ of the mean ocean $\delta^{18}O$ [*Waelbroeck et al.*, 2002]. The triple isotopic composition of ice and seawater falls on the meteoric water line of slope 0.528 in a $\ln(\delta^{17}O + 1) - \ln(\delta^{18}O + 1)$ plot [*Meijer and Li*, 1998; *Barkan and Luz*, 2005]. Thus the change of $\delta^{18}O$ by 1‰ is reflected by a change of 0.53‰ in $\delta^{17}O$ of the mean global ocean. These changes in $\delta^{17}O$ and $\delta^{18}O$ of the ocean are directly transmitted to the $\delta^{17}O$ and $\delta^{18}O$ of O_2 produced by oceanic photosynthesis.

5. Estimate of $^{17}\Delta_{terr}$

[16] We estimated global $^{17}\Delta_{terr}$ for the present and for the LGM in the following way. According to equation (1), $^{17}\Delta_{terr}$ is defined as

$$^{17}\Delta_{terr} = \ln\left(\frac{^{17}R_{terr}}{^{17}R_{atm}} + 1\right) - 0.516 \times \ln\left(\frac{^{18}R_{terr}}{^{18}R_{atm}} + 1\right), \quad (6)$$

where $^{18}R_{terr}$ and $^{17}R_{terr}$ are the isotopic ratios of O_2 produced by the terrestrial biosphere. These ratios depend on the fractionation during oxygen uptake and on the isotopic composition of the substrate water for photosynthesis, i.e., leaf water. As in previous studies [*Bender et al.*, 1994; *Blunier et al.*, 2002; *Hoffmann et al.*, 2004], we consider a steady state so that the flux during oxygen uptake is balanced by the corresponding O_2 flux released during photosynthesis. In this case, R_{terr} can be calculated as

$$^{*}R_{terr} = \frac{^{*}R_{lw}}{^{*}\alpha_{terr}}, \quad (7)$$

where "*" stands for 17 or 18, $^{*}R_{lw}$ is the global isotopic composition of leaf water, and $^{*}\alpha_{terr}$ stands for the global effective isotope fractionation factor associated with oxygen uptake. These two terms are estimated separately below.

5.1. Global Isotopic Composition of Leaf Water

[17] The most recent estimate of present global leaf water $\delta^{18}O$ (6–8‰) was obtained by *Gillon and Yakir* [2001]. For the LGM, *Blunier et al.* [2002] assumed that global $\delta^{18}O_{lw}$ has the same value as the present-day one. However, owing to the variations in climatic conditions and isotopic composition of the meteoric water consumed by plants between LGM and today, this assumption is not justified. Thus we redetermined global $\delta^{18}O_{lw}$ for the LGM. We estimated this value from the worldwide distributions of $\delta^{18}O_{lw}$ and photosynthetic O_2 flux. We multiplied for each region the local $\delta^{18}O_{lw}$ by the local O_2 flux, then summed the values for each region and normalized the final value by the global terrestrial photosynthetic O_2 flux.

[18] The local $\delta^{18}O_{lw}$ were obtained using the *Craig and Gordon* [1965] expression of evaporation applied to leaf water [*Dongmann et al.*, 1974; *Flanagan et al.*, 1991]. The Craig and Gordon approach states that $\delta^{18}O_{lw}$ depends on the isotopic composition of meteoric water, water vapor, relative humidity and temperature. From the latitudinal and seasonal variability of these input parameters (Appendix A), we produced monthly maps ($2° \times 2°$) of $\delta^{18}O_{lw}$. In Figures 1a and 1b we present the mean annual values of $\delta^{18}O_{lw}$ for the present and the LGM conditions. As can be seen, the spatial distribution of $\delta^{18}O_{lw}$ for both periods is roughly similar.

[19] The repartition of the photosynthesis fluxes was estimated as follows. Because vegetation is considered at steady state, the photosynthesis flux is equal to the sum of all O_2 uptake fluxes, i.e., of dark respiration, photorespiration and the Mehler reaction. Then, as detailed by *Hoffmann et al.* [2004], the worldwide repartition of the O_2 fluxes can be calculated from the distribution of the terrestrial Gross Primary Production (GPP), expressed in terms of carbon flux, and the distribution of the different plant types on Earth. Indeed, the proportion of plant types (C3, C4) greatly influences the rate of photorespiration and therefore the relationship between carbon and O_2 fluxes. As a rule, while C3 plants photorespire, C4 plants, under normal circumstances, do not. Moreover, the photorespiration flux varies among the different types of C3 plants. Thus, depending on the C3/C4 distribution, the repartition of O_2 fluxes can be significantly different from the one of carbon fluxes.

[20] We obtained the worldwide repartition of the GPP per unit surface for different biomes using the new dynamic global vegetation model ORCHIDEE (Organizing Carbon and Hydrology in Dynamic Ecosystems) integrating the most recent parameterizations of vegetation dynamics [*Krinner et al.*, 2005] (Appendix B). In this model, the variety of the biomes is expressed through 12 different plant functional types (PFT): two PFTs stand for the C4 plants and ten for the C3 plants. The competitive balance between C4 and C3 plants is driven by the growing season temperature and humidity as well as by CO_2 level.

[21] In Figures 2a and 2b, we present the total GPP (i.e., integrating the contribution of the 12 plant species) for

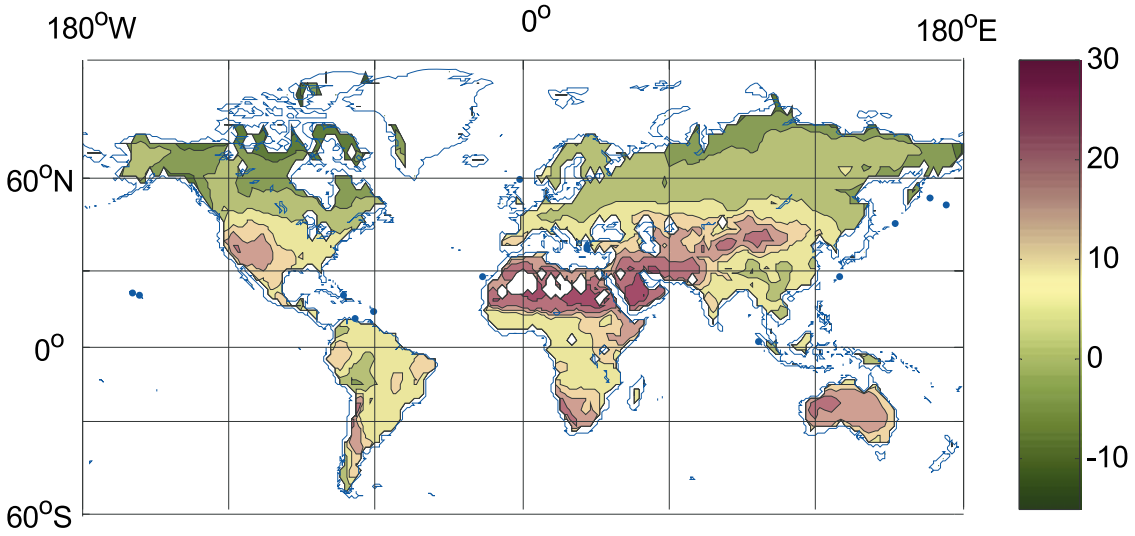

Figure 1a. Mean annual repartition of leaf water $\delta^{18}O$ (‰) for the present obtained with the Craig and Gordon approach.

present day and the LGM. As can be seen, there is a considerable decrease of GPP over the high latitudes in the Northern Hemisphere during the LGM due to the presence of large ice sheets. Thus the global $\delta^{18}O_{lw}$, which is transmitted to the atmospheric oxygen by photosynthesis, is less influenced by the high latitudes during the LGM than at present.

[22] In Figures 3a and 3b we show the distribution of the relative productivity of C4 plants for the present and the LGM, i.e., the distribution of the ratio between the GPP of C4 plants and the total GPP, obtained by the ORCHIDEE model. The high relative productivity of C4 plants in the LGM over Africa, Australia and South America implies a decrease of the O_2 flux over these regions due to low photorespiration. As a result, these regions had a relatively small influence on the global $\delta^{18}O_{lw}$. The distribution of the relative productivity of C3 plants can be directly derived from the maps on Figures 3a and 3b, since the sum of the relative productivities of both C3 and C4 plants equals one by definition.

[23] From the distributions of both total GPP and the relative productivity of different plant species, we constructed maps of the distribution of O_2 flux (details are given by *Farquhar et al.* [1980], *Lloyd and Farquhar* [1994], *von Caemmerer* [2000] and *Hoffmann et al.* [2004]).

[24] Lastly we calculated the global $\delta^{18}O_{lw}$ values as 7.0‰ and 8.0‰ for present day and LGM, respectively. The value for present day falls in the middle of the range proposed by *Gillon and Yakir* [2001]. The ~1‰ difference between the two periods is mainly due to the increase of the

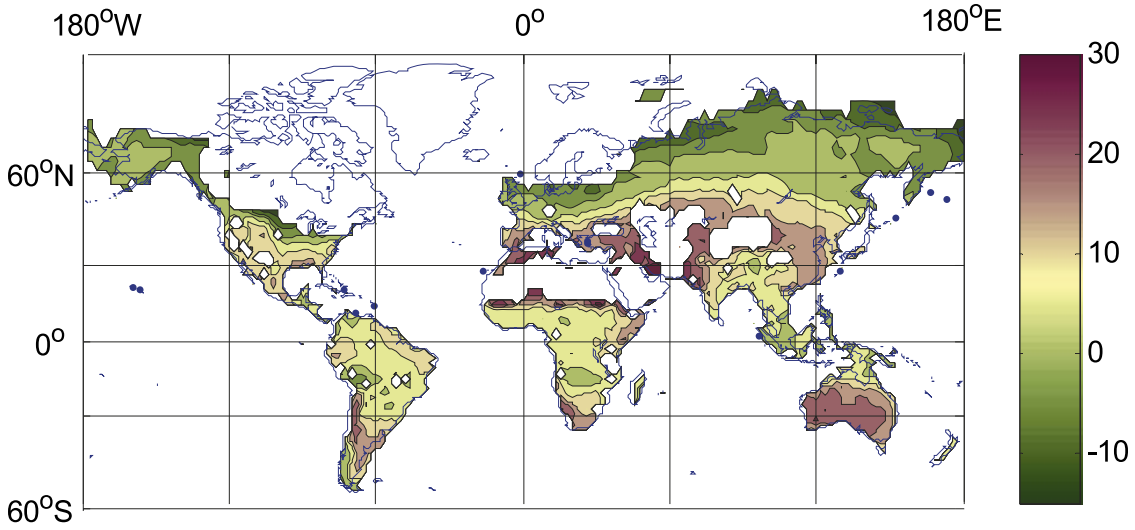

Figure 1b. Mean annual repartition of leaf water $\delta^{18}O$ (‰) for the LGM obtained with the Craig and Gordon approach.

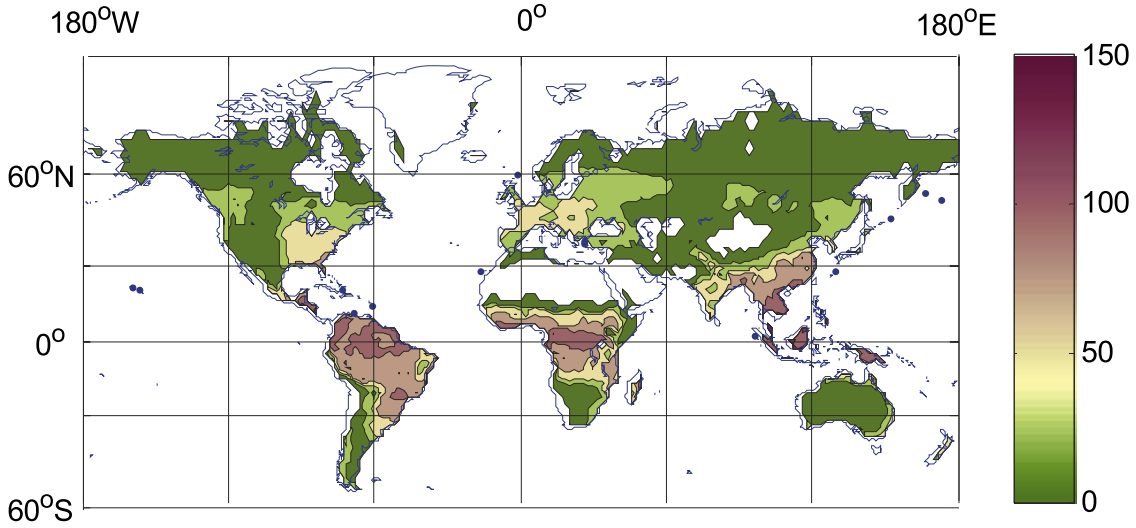

Figure 2a. Mean annual repartition of the total GPP for present day (gC d^{-1} m^{-2}) obtained from the ORCHIDEE model. The global GPP is 160 PgC yr^{-1}.

oxygen flux in the high latitudes between the LGM and present day owing to the reduction of the ice sheets (Figures 2a and 2b). Indeed, the plants consume meteoric water with a relatively low $\delta^{18}O$ in the high latitudes [*Edwards et al.*, 2002] such that $\delta^{18}O_{lw}$ is accordingly depleted (Figures 1a and 1b). Therefore an increase of the O_2 flux from the high latitudes vegetation results in a decrease of the global $\delta^{18}O_{lw}$.

[25] Until now there was no determination of leaf water $\delta^{17}O$ and the estimate of a global leaf water $\delta^{17}O$ for present day and the LGM was not possible. However, a recent study [*Landais et al.*, 2006] performed the first measurements of leaf water $\delta^{17}O$ over a various range of environmental conditions. They showed that the local $\delta^{17}O$ of leaf water may be calculated from the triple isotopic composition of oxygen in meteoric water and leaf water $\delta^{18}O$, as

$$\ln\left(\delta^{17}O_{lw}+1\right)=\ln\left(\delta^{17}O_{mw}+1\right)+\lambda_{transpi}\times\left[\ln\left(\delta^{18}O_{lw}+1\right)-\ln\left(\delta^{18}O_{mw}+1\right)\right], \quad (8)$$

where the subscripts "lw" and "mw" stand for leaf water and meteoric water, respectively, and $\lambda_{transpi}$ depends on the relative humidity, h, as [*Landais et al.*, 2006]

$$\lambda_{transpi}=0.522-0.008\times h, \quad (9)$$

when h is between 32 and 100%. For the very few regions with a relative humidity less than 32%, we assumed that

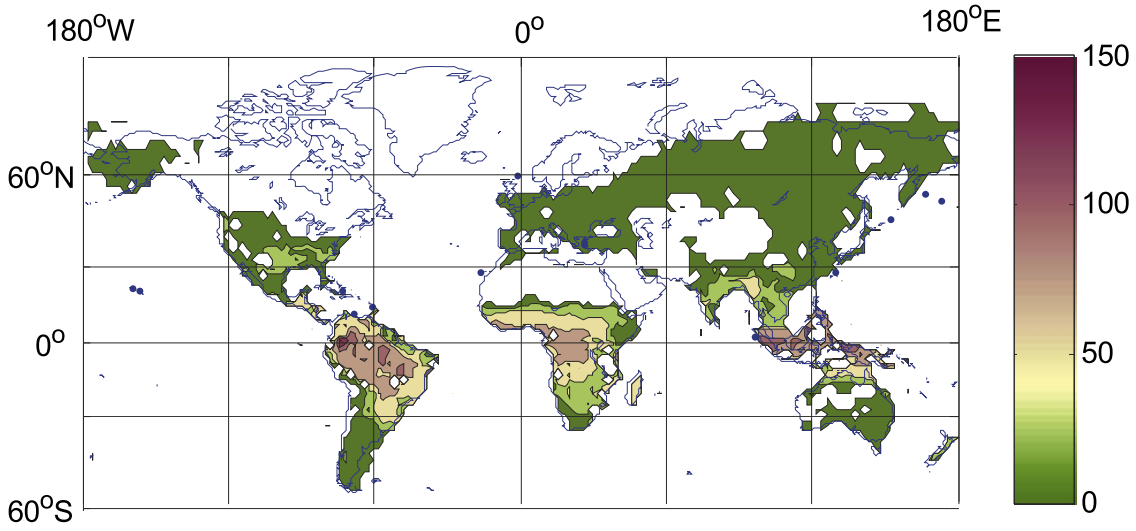

Figure 2b. Mean annual repartition of the total GPP for LGM (gC d^{-1} m^{-2}) obtained from the ORCHIDEE model. The global GPP is 110 PgC yr^{-1}.

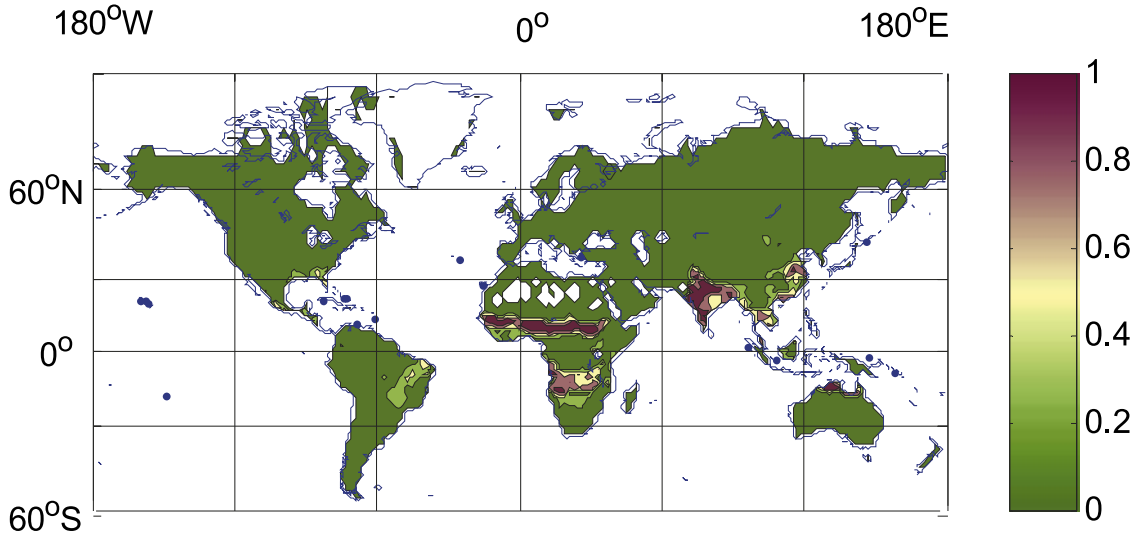

Figure 3a. Mean annual contribution of C4 plants to total GPP for present day as obtained from the ORCHIDEE model.

$\lambda_{transpi}$ is equal to 0.519. The $\delta^{17}O_{mw}$ is deduced for the given $\delta^{18}O_{mw}$ using the slope of 0.528 for the meteoric water line [*Meijer and Li*, 1998; *Barkan and Luz*, 2005].

[26] Using equations (8) and (9), we derived monthly maps of $\delta^{17}O_{lw}$ for present day and the LGM as it was done for $\delta^{18}O_{lw}$. Spatial and temporal integrations led to global $\delta^{17}O_{lw}$ values of 3.5‰ for present day and 4.1‰ for the LGM (Table 1).

5.2. Global Terrestrial Isotope Fractionation Factor

[27] We define the global isotope fractionation factor during terrestrial oxygen uptake by vegetation, α_{terr}, as the fractionation coefficients associated with the different O_2 uptake pathways (photorespiration, Mehler reaction, dark respiration in soil and in leaves) and express it as

$$^{*}\alpha_{terr} = {}^{*}\alpha_{photor} \times f_{photor} + {}^{*}\alpha_{Mehler} \times f_{Mehler} + {}^{*}\alpha_{dark\_soil} \times f_{dark\_soil} + {}^{*}\alpha_{dark\_leaves} \times f_{dark\_leaves}, \quad (10)$$

where "*" is 17 or 18; α_{photor}, α_{Mehler}, α_{dark_soil} and α_{dark_leaves} are the isotope fractionation factors associated with photorespiration, Mehler reaction and dark respiration in soil and in leaves, and f_{photor}, f_{Mehler}, f_{dark_soil} and f_{dark_leaves} are the corresponding fractions of the oxygen respiratory fluxes ($f_{photor} + f_{Mehler} + f_{dark\_soil} + f_{dark\_leaves} = 1$).

[28] *Blunier et al.* [2002] obtained values for $^{18}\alpha_{terr}$ of 0.9811 and 0.9809 for the present and the LGM, respectively. For this calculation they used a value for $^{18}\alpha_{Mehler}$ of 0.9849 obtained by *Guy et al.* [1993] while *Helman et al.* [2005] recently estimated it to be 0.9892. They also assumed a constant value for discrimination associated with dark respiration both in the soil and in the leaves as 0.982. However, *Angert et al.* [2003b] showed that the in situ ^{18}O discrimination associated with soil respiration is considerably weaker than in leaves and that the discrimination in soil varies between 10‰ and 22‰ among different vegetation types and, accordingly, among the different climatic regions. Thus we recalculated the values of $^{18}\alpha_{terr}$

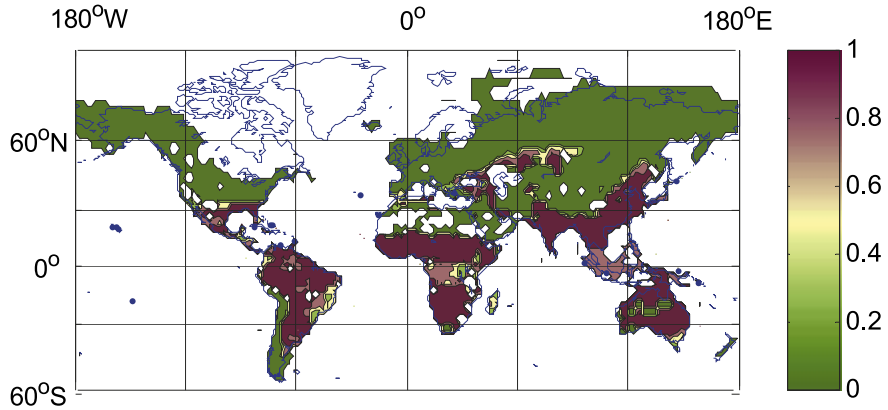

Figure 3b. Mean annual contribution of C4 plants to total GPP for LGM as obtained from the ORCHIDEE model.

Table 1. Estimates for the Present and the Last Glacial Maximum of the Different Parameters Involved in the Calculation of the Triple Isotopic Composition of Oxygen Issued From the Biosphere[a]

	PST	LGM
Global $\delta^{18}O_{lw}$ (‰/SMOW)	7.0 ± 1[b]	8.0 ± 1
Global $\delta^{17}O_{lw}$ (‰/SMOW)	3.5 ± 0.5	4.1 ± 0.5
f_{photor}	0.3	0.15
f_{Mehler}	0.1[c]	0.1[c]
f_{dark_soil}	0.44	0.55
f_{dark_leaves}	0.16	0.20
$^{18}\alpha_{photor}$	0.9786 ± 0.001[d]	0.9786 ± 0.001[d]
$^{18}\alpha_{Mehler}$	0.9892 ± 0.0002[d]	0.9892 ± 0.0002[d]
Global $^{18}\alpha_{dark\_soil}$	0.9844 ± 0.0005	0.9839 ± 0.0005
$^{18}\alpha_{dark\_leaves}$	0.981 ± 0.001	0.981 ± 0.001
λ_{photor}[e]	0.509 ± 0.001[d]	0.509 ± 0.001[d]
λ_{dark}[e]	0.516 ± 0.0004[f]	0.516 ± 0.0004[f]
λ_{Mehler}[e]	0.525 ± 0.002[d]	0.525 ± 0.002[d]
Global $^{18}\alpha_{terr}$	0.9826 ± 0.001	0.98306 ± 0.001
Global $^{17}\alpha_{terr}$	0.99101 ± 0.0005	0.99123 ± 0.0005
Global λ_{terr}[e]	0.5145 ± 0.0007	0.5156 ± 0.0006
$^{17}\Delta_{terrest}$ (permeg)	110 ± 35	140 ± 35
$^{17}\Delta_{ocean}$ (permeg)	249 ± 15[g]	261 ± 15

[a]PST, present; LGM, Last Glacial Maximum. Uncertainties are given for most of the parameters except for those derived from the ORCHIDEE model (see text).
[b]*Gillon and Yakir* [2001].
[c]*Bader et al.* [2000].
[d]*Helman et al.* [2005].
[e]Note that in work of *Helman et al.* [2005] the slope is given as $\lambda = (^{17}\alpha - 1)(^{18}\alpha - 1)$ for the one-way oxygen uptake processes. Here we deal with steady state (combination of O_2 uptake and mixing with photosynthetic O_2) so that $\lambda = \ln(^{17}\alpha)/\ln(^{18}\alpha)$ (details given by *Luz and Barkan* [2005]).
[f]*Angert et al.* [2003a].
[g]*Luz and Barkan* [2000].

taking into account the recent results by *Angert et al.* [2003b] and *Helman et al.* [2005] (Table 1; see details of calculations in Appendix C). The new values for the global $^{18}\alpha_{terr}$ are 0.9826 and 0.98306 for present day and for the LGM, respectively.

[29] The global $^{17}\alpha_{terr}$ was calculated from equation (10), where $^{17}\alpha_{photor}$, $^{17}\alpha_{Mehler}$ $^{17}\alpha_{dark\_soil}$ and $^{17}\alpha_{dark\_leaves}$ were obtained using the relationship [*Miller*, 2002; *Luz and Barkan*, 2005]

$$^{17}\alpha = \left(^{18}\alpha\right)^{\lambda}. \quad (11)$$

The corresponding values of $^{18}\alpha$ and λ as well as the resulting $^{17}\alpha_{terr}$ are given in Table 1.

[30] Finally, we obtained λ_{terr} as 0.5145 for present day and 0.5156 for the LGM. Sensitivity tests showed that the main uncertainty in λ_{terr} (0.0006–0.0007) is linked to the uncertainties in the slopes λ for the different processes [*Helman et al.*, 2005]. The other parameters included in equations (10) and (11) would modify λ_{terr} by less than 0.0002. It should be mentioned that, at first glance, λ_{terr} for present day and the LGM are statistically identical. However, because in the calculation of λ_{terr} for present day and the LGM the same values of λ are used for different processes, any increase/decrease of their values leads to a parallel increase/decrease of λ_{terr} for both present day and the LGM. Therefore the calculated decrease of λ_{terr} by 0.001 over the deglaciation is a firm result. It is a direct consequence of the larger fraction of C4 plants during the LGM than the present (Figures 3a and 3b); with more C4 plants the fraction of photorespiration associated with a low triple isotope slope (0.509) decreases and the resulting mean slope, λ_{terr}, increases.

6. Input Parameters

[31] In Table 1 we summarize all model parameters used in the calculations. The values for some of the parameters were taken from the literature, while the others were obtained in the present study.

7. Results and Discussion

7.1. The ^{17}O Anomalies for Present Day and LGM

[32] Using the model presented above, we calculated $^{17}\Delta_{ocean}$ for the LGM and $^{17}\Delta_{terr}$ for the present and the LGM as 261, 110 and 140 permeg, respectively. The associated uncertainties are detailed below.

[33] For $^{17}\Delta_{terr}$ our most disputable parameterization choice was the relationship used to infer humidity and temperature during photosynthesis (Appendix A). A change in humidity by 5% leads to ^{18}O enrichment of the global leaf water by 1‰ or more. Thus for the present day the calculated $\delta^{18}O_{lw}$ becomes higher than 8‰, which is in disagreement with the data of *Gillon and Yakir* [2001]. Therefore we consider 5% as the maximum uncertainty associated with humidity. Sensitivity tests have shown that such change in humidity affects $^{17}\Delta_{terr}$ only by 4 permeg. For temperature, modifications by 3°C, corresponding to the maximal uncertainties in classical temperature reconstructions (http://www.ncdc.noaa.gov/paleo/recons.html), lead to changes in $^{17}\Delta_{terr}$ that are less than 4 permeg.

[34] Another important assumption in our model concerns the fraction of the Mehler reaction in the total flux of oxygen into the biosphere. As the slope of the biological steady state associated with the Mehler reaction is relatively high, a change in the proportion of the Mehler reaction will increase/decrease the $^{17}\Delta_{terr}$. We realize that the value of 0.1 given by *Bader et al.* [2000] is not necessarily representative of the global terrestrial biosphere but, to the best of our knowledge, there are no other estimates of this parameter. Sensitivity tests showed that the variations up to 70% in f_{Mehler} lead to an uncertainty of 10 permeg in $^{17}\Delta_{terr}$, which corresponds to the usual analytical precision [*Barkan and Luz*, 2003, 2005].

[35] Lastly, the accuracy of $^{17}\Delta_{terr}$ depends on the correctness of different slopes, λ, which are usually determined with a precision around 0.001 (Table 1). These uncertainties introduce a total error in $^{17}\Delta_{terr}$ of ~20 permeg.

[36] We did sensitivity experiments modifying randomly the relationships used to obtain temperature and relative humidity, the proportion of the Mehler reaction and the slopes of the different processes involved in the terrestrial biosphere productivity (the other uncertainties presented on Table 1 have negligible effects on $^{17}\Delta_{terr}$) and found that the maximal error for $^{17}\Delta_{terr}$ is 35 permeg. This uncertainty is relatively high, but it should be mentioned that when we modify any basic assumption in our model, we shift in a

Table 2. The $^{17}\Delta_{bio}$ for the LGM and Present Day (PST) and the Resulting Ratios $F_{bio,LGM}/F_{bio,PST}$[a]

$F_{O,PST}/F_{T,PST}$[b]	$^{17}\Delta_{bio,PST}$	$F_{O,LGM}/F_{T,LGM}$[c]	$^{17}\Delta_{bio,LGM}$	$F_{bio,LGM}/F_{bio,PST}$
0.45	124[d]	0.56	156	0.75
		1.08	178	0.73
	182[e]	0.56	211	0.73
		1.08	227	0.67
0.59	145[d]	0.73	177	0.73
		1.41	205	0.60
	189[e]	0.73	217	0.74
		1.41	234	0.67

[a]Only extreme values given.
[b]Minimum and maximum values [*Bender et al.*, 1994; *Blunier et al.*, 2002; *Hoffmann et al.*, 2004].
[c]Minimum and maximum values calculated from the corresponding values of $F_{O,PST}/F_{T,PST}$ and extreme values of $F_{O,LGM}/F_{O,PST}$ (1.0–1.1) and $F_{T,LGM}/F_{T,PST}$ (0.5–0.8) as given in the main text.
[d]This value estimated with equation (5) using the minimum values for $^{17}\Delta_{terr}$ and $^{17}\Delta_{ocean}$.
[e]This value estimated with equation (5) using the maximum values for $^{17}\Delta_{terr}$ and $^{17}\Delta_{ocean}$.

similar way both $^{17}\Delta_{terr,LGM}$ and $^{17}\Delta_{terr,PST}$ so that the difference between them, 30 permeg, remains constant.

[37] The uncertainty in $^{17}\Delta_{ocean,LGM}$ results from the uncertainties in the LGM global sea level $\delta^{18}O$ and $^{17}\Delta_{ocean,PST}$. The uncertainty associated with the first term is less than 0.1‰, and has a negligible effect on $^{17}\Delta_{ocean,LGM}$. Thus $^{17}\Delta_{ocean,LGM}$ has the same uncertainty as $^{17}\Delta_{ocean,PST}$. This means that if $^{17}\Delta_{ocean,PST}$ is over(under)-estimated by 15 permeg, the same applies to $^{17}\Delta_{ocean,LGM}$, and the difference between $^{17}\Delta_{ocean,PST}$ and $^{17}\Delta_{ocean,LGM}$ remains constant as 12 permeg.

[38] Our discussion does not include the uncertainties associated with the ORCHIDEE model, which are very difficult to estimate as with every biosphere model. However, outputs of this model show a good agreement with the present vegetation [*Krinner et al.*, 2005]. Furthermore, *Lathiere* [2005] did a detailed comparison between available vegetation paleodata [*Ray and Adams*, 2001] and ORCHIDEE outputs for the LGM. It was shown that although the PFT of ORCHIDEE are based on present-day vegetation, there is a good agreement between maps of LGM vegetation obtained from the model and from paleodata.

[39] As stated in section 3.1 (equation (5)), $^{17}\Delta_{bio}$ varies with the relative proportions of oceanic to terrestrial oxygen productivities. For present day, F_O/F_T was given within the range of 0.45 to 0.59 by several authors [*Bender et al.*, 1994; *Blunier et al.*, 2002; *Hoffmann et al.*, 2004]. For the LGM we used the ORCHIDEE model and found that F_T was 54% of the present-day value. From two other terrestrial biosphere models (CARAIB [*Francois et al.*, 1998] and BIOME [*Haxeltine and Prentice*, 1996]), *Blunier et al.* [2002] found that F_T during the LGM was 50–80% of the present value. On the basis of these results, we accepted 50–80% as the maximum range of F_T variations between the LGM and the present day. To evaluate the oceanic fluxes F_O, we assumed that F_O varied proportionally to oceanic productivity. While *Bopp et al.* [2003] found no change in oceanic productivity between the LGM and the present, G. Hoffmann and E. Maier-Reimer (personal communication, 2006) modeled oceanic productivity that was 20% higher in the LGM than the present. The latter result is in agreement with the reviews by *Bender et al.* [1994] and *Kohfeld et al.* [2005], suggesting a worldwide decrease of the oceanic productivity and export production between the LGM and present day. Because the accuracy of each estimate is subject to discussion, we used both of them as extreme values in our study. Finally, on the basis of different values of $F_{T,LGM}/F_{T,PST}$ and $F_{O,LGM}/F_{O,PST}$, we obtained the ratio F_O/F_T for the LGM as a function of the ratio F_O/F_T for the present. $F_{O,LGM}/F_{T,LGM}$ varies between 0.56 and 1.41 (Table 2).

[40] It should be mentioned that it is tempting to use the Dole effect approach for estimating the change in F_O/F_T between the present and the LGM [e.g., *Bender et al.*, 1994; *Hoffmann et al.*, 2004]. According to this approach the magnitude of the Dole effect should decrease as F_O/F_T increases. However, the magnitude of the Dole effect during the LGM was similar to the present value [*Bender et al.*, 1994; *Malaizé et al.*, 1999], despite ample evidence for considerable change in terrestrial primary productivity. As discussed by *Hoffmann et al.* [2004] the magnitude of the Dole effect depends, in addition to F_O/F_T, also on other factors such as latitudinal shifts in precipitation that resulted in different $\delta^{18}O$ of meteoric water used by the terrestrial vegetation in the temperate zone. Therefore we cannot use the change in the Dole effect as a measure of the F_O/F_T difference between the present and the LGM.

[41] Values of $^{17}\Delta_{bio}$ for present day and the LGM were calculated using equation (5). As can be seen, the uncertainties in $^{17}\Delta_{bio}$ depend on uncertainties in the F_O/F_T ratio, $^{17}\Delta_{terr}$ and $^{17}\Delta_{ocean}$. In Table 2 we present estimates of $^{17}\Delta_{bio}$ obtained for the maximum and minimum values of F_O/F_T, taking into account the maximum uncertainties in $^{17}\Delta_{terr}$ and $^{17}\Delta_{ocean}$. It is important to note that the uncertainties in $^{17}\Delta_{bio,LGM}$ and $^{17}\Delta_{bio,PST}$ are not independent because, as discussed above, $^{17}\Delta_{terr,LGM}$ is always 30 permeg higher than $^{17}\Delta_{terr,PST}$ and $^{17}\Delta_{ocean,LGM}$ is 12 permeg higher than $^{17}\Delta_{ocean,PST}$. We end up with a present-day estimate of $^{17}\Delta_{bio}$ of 124–189 permeg for present and 156–234 permeg for the LGM.

[42] As can be seen from Table 2, there is a general decrease of $^{17}\Delta_{bio}$ between the LGM and present day. With the aim of understanding the cause of this phenomenon, we present a scheme in Figure 4 that explains how the temporal variation of $^{17}\Delta_{bio}$ results from the difference in the relationships between $\delta^{17}O$ and $\delta^{18}O$ among the various processes, and from the spatial repartition of vegetation and isotopic composition of meteoric water.

[43] We first focus on the anomaly associated with the oceanic biosphere, $^{17}\Delta_{ocean}$. Point A accounts for the isotopic composition of the global ocean today. From this point, production of O_2 by photosynthesis and marine respiration at the biological steady state leads to point B, representing the isotopic composition of oxygen issued from the ocean and characterized by a $^{17}\Delta_{ocean}$ of 249 permeg [*Luz and Barkan*, 2000]. For the LGM, the larger ice sheets imply that $\delta^{18}O$ of the global ocean at LGM is 1‰ higher than the present-day oceanic $\delta^{18}O$

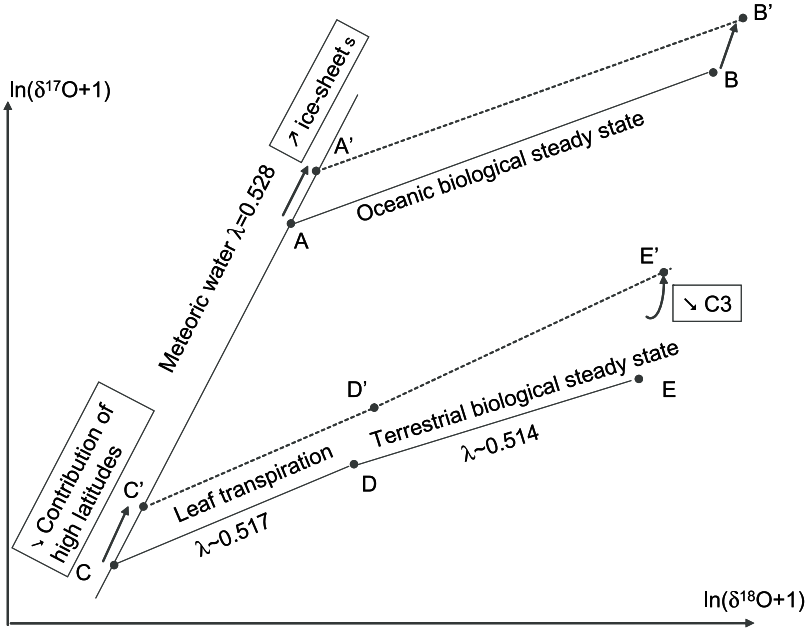

Figure 4. Scheme showing the relative positions of the isotopic composition of global ocean (A for present day, A′ for the LGM), oxygen issued from oceanic productivity (B for present day, B′ for the LGM), mean meteoric water (C for present day, C′ for the LGM), mean leaf water (D for present day, D′ for the LGM), and oxygen issued from terrestrial productivity (E for present day, E′ for the LGM).

[*Waelbroeck et al.*, 2002], and thus point A is shifted to point A′. This shift is driven along the meteoric water line of slope 0.528, i.e., larger than 0.516, so that $^{17}\Delta$ in point A' is greater than in point A. Since we assume no change in the slope of the oceanic biological steady state between the LGM and present day (section 4), the shift from A to A′ is reflected by a similar shift from B to B′, the point representing the isotopic composition of oxygen issued from the ocean at LGM. As a result, $^{17}\Delta_{ocean,LGM}$ is larger than $^{17}\Delta_{ocean,PST}$ by 12 permeg.

[44] We now concentrate on the anomaly associated with the terrestrial biosphere, $^{17}\Delta_{terr}$. The mean annual meteoric water isotopic composition consumed by the plants is shown by point C. From this point, transpiration in leaves leads to the isotopic composition of leaf water represented by point D. We estimated the mean slope of this line (CD) for present-day conditions as 0.517. From point D, production of O_2 by photosynthesis and oxygen uptake leads to point E, representing the isotopic composition of oxygen emanating from the terrestrial biosphere and characterized by a $^{17}\Delta_{terr}$ of 110 permeg today. The slope of the line (DE) is influenced by the relative proportions of the different respiration processes (section 5.2 and Table 1). For present-day conditions we calculated the mean slope associated with terrestrial biological steady state, λ_{terr}, as 0.514.

[45] During the LGM, the ice sheets extent reduces the biosphere productivity in the high latitudes (Figures 2a and 2b). These regions are associated with low $\delta^{18}O$ of the meteoric water [*Edwards et al.*, 2002] and therefore the ice sheet extent leads to an increase of the mean $\delta^{18}O$ of meteoric water consumed during photosynthesis for the LGM as compared to present day. Using the spatial and seasonal repartition of oxygen fluxes associated with photosynthesis (section 5.1) and of the meteoric water $\delta^{18}O$ for both the LGM and present day, we calculated this increase as 1.2‰. By definition, C lies on the meteoric water line with the slope 0.528 [*Meijer and Li*, 1998]. Thus the corresponding change of $\delta^{17}O$ shifts point C to C' along the line with a slope higher than 0.516, and this results in an increase of $^{17}\Delta_{terr}$ by ~15 permeg.

[46] We then evaluated the mean relative humidity during photosynthesis through a spatial and annual weighted average by the oxygen biosphere productivity and found that this mean relative humidity was not considerably different in the LGM than at present. Therefore the slope of the line accounting for the leaf transpiration process is roughly the same for the LGM and present day, and the change in the leaf water isotopic composition from D to D′ mainly reflects the shift from C to C′. Finally, the contribution of C3 plants to the total biosphere productivity is far less important during the LGM than the present (Figures 3a and 3b) and, despite the higher photorespiration of these plants during the LGM compared to today, the total effect is that the photorespiration flux is lower during the LGM than today. Because photorespiration is associated with a relatively small slope (0.509), the slope of the line accounting for global terrestrial biological steady state during the LGM (D′E′) is larger than the one accounting for present-day conditions (DE). This leads to an additional increase of $^{17}\Delta_{terr,LGM}$ (point E′) with respect to $^{17}\Delta_{terr,PST}$ (point E) by another 15 permeg.

7.2. Increase in Global Plant Productivity Since the LGM

[47] On the basis of the obtained $^{17}\Delta_{bio}$ in the LGM and the present, we calculated using equation (4) the rate of

global biological productivity during the LGM as 60–75% of the present rate (Table 2).

[48] *Blunier et al.* [2002] with their model for interpreting the triple isotopic composition of oxygen, obtained that $F_{bio,LGM}$ is 80 ± 4% of $F_{bio,PST}$. Note that the given uncertainty only accounts for the uncertainty of $F_{T,LGM}/F_{T,PST}$. As discussed above, these authors used the same slope for the different relationships between $\delta^{17}O$ and $\delta^{18}O$ associated with biosphere productivity, and this assumption leads to a 4% overestimation of the ratio $F_{bio,PST}/F_{bio,LGM}$. In addition, Blunier et al. did not consider the seasonal and spatial distributions of vegetation and isotopic composition of meteoric water between the LGM and present day. Our calculations showed that this simplification can explain another part of the overestimation of $F_{bio,PST}/F_{bio,LGM}$ obtained by these authors.

[49] The LGM productivity obtained in the present study is at the lowest end of the previous estimates from different oceanic [*Bopp et al.*, 2003; G. Hoffmann and E. Maier-Reimer, personal communication, 2006] and terrestrial (BIOME, CARAIB, ORCHIDEE) biosphere models: 65–95%. It thus suggests that the change in the global biosphere over the last deglaciation was larger than previously thought.

[50] Finally, our constraint on the LGM biosphere productivity can be used as an additional and independent tool to test the numerous vegetation models recently developed [e.g., *Francois et al.*, 1998; *Friedlingstein et al.*, 1992; *Kaduk and Heimann*, 1996; *Krinner et al.*, 2005]. Until now, such models were tested through a comparison between the simulated change of vegetation over the deglaciation and local paleodata of vegetation [e.g., *Ray and Adams*, 2001; *Harrison and Prentice*, 2003]. Here we propose comparing the changes in biosphere productivity over the deglaciation obtained from our budget of three oxygen isotopes and the one calculated by biosphere models. As an illustration, the ORCHIDEE, BIOME and CARAIB models give values for $F_{bio,LGM}/F_{bio,PST}$ of 0.72 ± 0.05, 0.70 ± 0.05 and 0.90 ± 0.05, respectively, assuming a ratio $F_{ocean,LGM}/F_{ocean,PST}$ of 1.10 ± 0.1 as in our study [*Bopp et al.*, 2003; G. Hoffmann and E. Maier-Reimer, personal communication, 2006]. Our estimate, 0.60–0.75, supports the use of the BIOME and ORCHIDEE models to study the interaction between biosphere and climate over the deglaciation.

8. Conclusions

[51] We have presented a global model to infer the past biosphere productivity from the record of the triple isotopic composition of atmospheric oxygen. This model incorporates the recently determined relationships between $\delta^{17}O$ and $\delta^{18}O$ in the biological and hydrological cycles as well as the spatial and seasonal variations of vegetation distribution, climatic conditions and isotopic composition of meteoric water. On the basis of this model, we provide the best possible global estimates for LGM and present day of: leaf water triple isotopic composition, isotopic fractionation factors for terrestrial dark respiration in soils and in leaves and total terrestrial respiration, relationships between $\delta^{17}O$ and $\delta^{18}O$ associated with terrestrial biological steady state, and ^{17}O anomalies issued from the both terrestrial and oceanic biospheres.

[52] Using three oxygen isotope budget calculations and the vegetation distribution simulated by the ORCHIDEE model, we evaluated the global oxygen biospheric productivity of the LGM as 60–75% of the present value. Our result is based on using the ORCHIDEE model, and it is possible that new and more powerful vegetation models might require us to reconsider our conclusion. However, the 30 permeg difference in ^{17}O anomalies between the LGM and the present is explained mostly by the different ice sheet extensions and the C3/C4 distributions. These differences between the LGM and the present are confirmed by paleodata [*Ray and Adams*, 2001; *Clark and Mix*, 2002], and we therefore do not expect a considerable change in the given value.

[53] Our value is at the lower end of previous estimates and suggests that the difference in biosphere productivity between the LGM and the present is larger than previously thought. The obtained result has an important implication for evaluating the performances of biosphere models. Further studies on the long-term records of the triple isotopic composition of atmospheric oxygen are necessary to better understand the link between climate and biosphere productivity over different climatic transitions.

Appendix A: Input Parameters for Calculation of Leaf Water $\delta^{18}O$

A1. Source Water and Water Vapor $\delta^{18}O$

[54] The current distribution of $\delta^{18}O$ in meteoric water has been mapped from the GNIP network [*Edwards et al.*, 2002]. For the LGM, estimates of the isotopic composition of meteoric water are very rare except over the Polar Regions. Sparse local reconstructions suggest that the $\delta^{18}O$ of meteoric water during the LGM was 2–4‰ lower than today in temperate Europe [*von Grafenstein et al.*, 1999; *Navarro et al.*, 2004] and similar to today in tropical America [*Mora and Pratt*, 2001; *Chowdhury et al.*, 2004]. *Jouzel et al.* [2000] modeled a worldwide repartition of $\delta^{18}O$ in meteoric water for the LGM that is in agreement with the aforementioned available local data. We therefore used, for our LGM calculations, the map of meteoric water $\delta^{18}O$ from *Jouzel et al.* [2000].

[55] We calculated the difference in $\delta^{18}O$ between the water vapor and the meteoric water with the atmospheric general circulation model, ECHAM, including the isotopes in the hydrological cycle [*Hoffmann et al.*, 1998] for the LGM and for the present.

A2. Climatic Conditions: Temperature and Relative Humidity

[56] The present-day climate conditions (monthly mean relative humidity and temperature at 2 m) are based on climate forcing from CRU (Climate Research Unit, UK) with relative humidity corrected using ECMWF (European Centre for Medium-Range Weather Forecasts, UK) data. Concerning the LGM, monthly mean relative humidity and temperature are based on the present forcing corrected by the corresponding anomalies simulated with the LMDz (Laboratoire de Météorologie Dynamique) general circulation

model [*Harzallah and Sadourny*, 1995] considering LGM atmospheric CO_2 concentration [*Poutou et al.*, 2004]. Note that the climatic fields issued from the last version of LMDz, traditionally used to force the ORCHIDEE mode, are very close to those simulated by the ECHAM model even at high latitudes where general circulation models often disagree.

[57] The aforementioned spatial fields of temperature and humidity are monthly averages and integrate night and day values. However, photosynthesis occurs only during the day, i.e., with a higher temperature and a lower relative humidity than the monthly averages. The isotopic composition of leaf water transmitted to the atmospheric oxygen hence corresponds to day conditions and not to monthly averages. In order to calculate temperature and humidity corresponding to day conditions from monthly averages, we followed the approach by *Lloyd and Farquhar* [1994] and *Hoffmann et al.* [2004]. Leaf temperature during photosynthesis, T_l, was related to the monthly mean air temperature, T_m (in °C), through $T_l = 1.05 \times (T_m + 2.5)$. The mean humidity was obtained by multiplying the monthly average humidity by a coefficient, C_h, less than 1. C_h was adjusted to 0.85 so that the global mean annual average for our modeled leaf water $\delta^{18}O$ matches the determination by *Gillon and Yakir* [2001] who obtained a global leaf water $\delta^{18}O$ between 6 and 8‰ for the present.

Appendix B: GPP Distributions for Different Plant Species—ORCHIDEE Model

[58] The ORCHIDEE model considers 12 different plant functional types (PFT) among which two are C4 plants and ten are C3 plants. For the present, the vegetation distribution was prescribed with global maps based on the work by *Loveland et al.* [2000], corrected by *Ramankutty and Foley* [1999] and by *Goldewijk* [2001] for crops and grasses. The repartition of the vegetation for the LGM resulted from a model simulation: It starts with bare soil and runs 500 years using the corrected LGM climate, orbital parameters and atmospheric CO_2 until equilibrium is reached. Emerged land due to the sea level decrease was taken into account. The resulting worldwide repartition of vegetation shows a good agreement with observations for the present [*Krinner et al.*, 2005] and with the compilation of paleodata for the LGM by *Ray and Adams* [2001].

[59] The GPP per unit surface was determined for each grid point and each of the 12 PFT, through a coupled photosynthesis and water balance directly included in the ORCHIDEE model [*Krinner et al.*, 2005]. Combining these results with the vegetation distribution, we calculated the distribution of the GPP for the 12 plant species. The distribution of the GPP for the C4 plants is then directly obtained by adding the GPP distributions of the two PFT standings for C4 plants. Similarly, adding the GPP distributions of the ten remaining PFTs gives the distribution of GPP for the C3 plants. Adding up both C3 and C4 plants gives the distribution of the total GPP.

Appendix C: Calculation of $^{18}\alpha_{terr}$

[60] The calculation of $^{18}\alpha_{terr}$ is done using equation (10); we outline below how we estimated each parameter involved in equation (10).

[61] Because there is no information on variations of f_{Mehler} among different plant species, we assumed that f_{Mehler} is independent of the spatial and seasonal distributions of vegetation. In the present study we followed *Bader et al.* [2000] and took a constant f_{Mehler} of 0.1. In contrast, f_{photor} depends on the type of vegetation cover (especially on the ratio of C3/C4 plants). The worldwide distribution of f_{photor} was therefore derived from the distributions of the relative productivity of each group of plant species given by the ORCHIDEE model. A consequent integration gave the values for global f_{photor} of 0.3 and 0.15 for the present and the LGM, respectively. The difference in photorespiration fraction between the LGM and the present is linked to the substantial decrease of C4 plants since the last glacial because C4 plants do not photorespire under normal conditions. It should be pointed out that the shift from C4 to C3 domination masks the effect of increased photorespiration fraction in the remaining C3 plants due to lower CO_2 concentration during the LGM.

[62] *Schlesinger and Andrews* [2000] have recently proposed that the modern global carbon flux of soil respiration is 63% of the global GPP. Using the present-day vegetation distribution from the ORCHIDEE model, we converted this estimate from carbon flux to oxygen flux, and obtained the present-day global O_2 soil respiration flux as 44% of the global oxygen productivity. Then f_{dark_leaves} was calculated as 0.16 (= 1-0.1-0.3-0.44). For the LGM, in the absence of any available estimate for the proportion of soil respiration, we used the same ratio $f_{dark\_leaves}/f_{dark\_soil}$ of 0.16/0.44 and, given the fractions of photorespiration and Mehler reaction, we obtained values of 0.55 and 0.20, respectively, for f_{dark_soil} and f_{dark_leaves}.

[63] The fractionation factors, $^{18}\alpha$, for photorespiration and Mehler reaction have recently been determined by *Helman et al.* [2005] and are given in Table 1. For estimating the global $^{18}\alpha_{dark\_soil}$, we first plotted its spatial variability. With this aim, we used the distribution of the vegetation types derived by the ORCHIDEE model and attributed to each vegetation type the appropriate value of soil isotope discrimination by respiration given by *Angert et al.* [2003b]. Then, to integrate this distribution, we took into account the different rates of soil respiration in climatic regions. This was calculated from the distribution of the global oxygen uptake flux (section 5.1), and from the distribution of f_{dark_soil} (calculated from the vegetation distribution to have the proportion of photorespiration in the same way that we obtained the global f_{dark_soil}). Finally, combining the distributions of the global oxygen uptake flux, f_{dark_soil} and $^{18}\alpha_{dark\_soil}$, we integrated over the vegetated areas and obtained the global values for $^{18}\alpha_{dark\_soil}$ as 0.9844 for present day and 0.9839 for the LGM. Our sensitivity tests showed that the maximum possible error in the global $^{18}\alpha_{dark\_soil}$ due to possible uncertainties in the relative proportions of dark respiration in soils and leaves is ±0.0005.

[64] For estimating $^{18}\alpha_{dark\_leaves}$, we followed *Angert et al.* [2003a] assuming that 10% of the dark respiration is through the AOX (alternative oxidase pathway) and 90% through the COX (cytochrome oxidase pathway). Then, using the fractionation factors of AOX ($^{18}\alpha$ = 0.97

[*Ribas-Carbo et al.*, 2000]) and of COX ($^{18}\alpha = 0.982$ [*Guy et al.*, 1989, 1993]), we obtained a constant value for $^{18}\alpha_{dark\_leaves}$ as 0.981. Using equation (10) we calculated the global $^{18}\alpha_{terr}$ as 0.9826 for present day and 0.98306 for the LGM. The smaller fraction of photorespiration during the LGM than at present explains why $^{18}\alpha_{terr}$ is larger for the LGM than now, while the evolution of $^{18}\alpha_{dark\_soil}$ was the opposite. Finally, taking into account the uncertainties in $^{18}\alpha_{dark\_soil}$, $^{18}\alpha_{photor}$, $^{18}\alpha_{Mehler}$ and in the proportion of COX and AOX, the maximum error on $^{18}\alpha_{terr}$ is about ±0.001.

[65] **Acknowledgments.** We would like to acknowledge Georg Hoffmann, Gerhardt Krinner, and Pierre Friedlingstein for helpful discussions. We are very grateful to the associated editor Corinne Le Quere and one anonymous reviewer whose comments contributed to significantly improving this paper. B. L. thanks the Israel Science Foundation (grant 188/03-13.0) for supporting of this research. A. L. was also supported by fellowships from the Lady Davis Foundation and the European Marie Curie grant (MEIF-CT-2005-023822). The work of J. L. was supported by the European project ENSEMBLES (GOCE-CT-2003-505539).

References

Angert, A., S. Rachmilevitch, E. Barkan, and B. Luz (2003a), Effects of photorespiration, the cytochrome pathway, and the alternative pathway on the triple isotopic composition of atmospheric O_2, *Global Biogeochem. Cycles*, *17*(1), 1030, doi:10.1029/2002GB001933.

Angert, A., et al. (2003b), Contribution of soil respiration in tropical, temperate, and boreal forests to the ^{18}O enrichment of atmospheric O_2, *Global Biogeochem. Cycles*, *17*(3), 1089, doi:10.1029/2003GB002056.

Bader, M. R., S. von Caemmerer, S. Ruuska, and H. Nakano (2000), Electron flow to oxygen in higher plants and algae: Rates and control of direct photoreduction (Mehler reaction) and rubisco oxygenase, *Philos. Trans. R. Soc., Ser. B*, *355*, 1433–1445.

Barkan, E., and B. Luz (2003), High-precision measurements of O-17/O-16 and O-18/O-16 of O-2 and O-2/Ar ratio in air, *Rapid Commun. Mass Spectrom.*, *17*, 2809–2814.

Barkan, E., and B. Luz (2005), High precision measurements of O-17/O-16 and O-18/O-16 of O_2 in H_2O, *Rapid Commun. Mass Spectrom.*, *19*, 3737–3742.

Barnola, J. M., D. Raynaud, Y. S. Korotkevich, and C. Lorius (1987), Vostok ice core provides 160,000-year record of atmospheric CO_2, *Nature*, *329*, 408–414.

Bender, M., T. Sowers, and L. D. Labeyrie (1994), The Dole effect and its variation during the last 130,000 years as measured in the Vostok core, *Global Biogeochem. Cycles*, *8*(3), 363–376.

Blunier, T., B. Barnett, M. L. Bender, and M. B. Hendricks (2002), Biological oxygen productivity during the last 60,000 years from triple oxygen isotope measurements, *Global Biogeochem. Cycles*, *16*(3), 1029, doi:10.1029/2001GB001460.

Bopp, L., K. E. Kohfeld, C. Le Quéré, and O. Aumont (2003), Dust impact on marine biota and atmospheric CO_2 during glacial periods, *Paleoceanography*, *18*(2), 1046, doi:10.1029/2002PA000810.

Chowdhury, A. H., C. Ridgeway, and R. E. Mace (2004), Origin of the waters in the San Solomon Spring system, Trans-Pecos, Texas, in *Aquifers of the Edwards Plateau, Texas Water Dev. Board Rep. 360*, edited by R. E. Mace et al., pp. 315–344, Texas Water Dev. Board, Austin, Tex.

Clark, P. U., and A. C. Mix (2002), Ice sheets and sea level of the Last Glacial Maximum, *Quat. Sci. Rev.*, *21*, 1–7.

Craig, H., and L. Gordon (1965), Deuterium and oxygen-18 in the ocean and the marine atmosphere, in *Proceedings: Stable Isotopes in Oceanographic Studies and Paleotemperatures. Conferences in Nuclear Geology*, edited by E. Tongiorgi, pp. 9–130, Cons. Naz. Delle Ric. Lab. di Geol. Nucl., Pisa, Italy.

Dongmann, G., H. W. Nuernberg, H. Foerstel, and K. Wagener (1974), On the enrichment of $H_2^{18}O$ in the leaves of transpiring plants, *Radiat. Environ. Biophys.*, *11*, 41–52.

Edwards, T. W. D., S. J. Birks, and J. J. Gibson (2002), Isotope tracers in global water and climate studies of the past and present: International Conference on the Study of Environmental Change Using Isotope Techniques, *IEAA-CN-80/66*, Int. Atom. Energy Agency, Vienna.

Farquhar, G. D., S. von Caemmerer, and J. A. Berry (1980), A biochemical model of photosynthetic CO_2 assimilation in leaves of C3 species, *Planta*, *149*, 78–90.

Flanagan, L. B., J. D. Marshall, and J. R. Ehleringer (1991), Comparison of modeled and observed environmental influences on the stable oxygen and hydrogen isotope composition of leaf water in *Phaseolus vulgaris* L., *Plant Physiol.*, *96*, 623–631.

Francois, L. M., C. Delire, P. Warnant, and G. Munhoven (1998), Modelling the glacial-interglacial changes in the continental biosphere, *Global Planet. Change*, *17*, 37–52.

Friedlingstein, P., C. Delire, J.-F. Muller, and J.-C. Gerard (1992), The climate induced variation of the continental biosphere: A model simulation of the Last Glacial Maximum, *Geophys. Res. Lett.*, *19*, 897–900.

Gillon, J., and D. Yakir (2001), Influence of carbonic anhydrase activity in terrestrial vegetation on the ^{18}O content of atmospheric CO_2, *Science*, *291*, 2584–2587.

Goldewijk, K. K. (2001), Estimating global land use change over the past 300 years: The HYDE Database, *Global Biogeochem. Cycles*, *15*(2), 417–433.

Guy, R. D., J. A. Berry, M. L. Fogel, and T. C. Hoering (1989), Differential fractionation of oxygen isotopes by cyanide-resistant and cyanide-sensitive respiration in plants, *Planta*, *177*, 483–491.

Guy, R. D., M. L. Fogel, and J. A. Berry (1993), Photosynthetic fractionation of the stable isotopes of oxygen and carbon, *Plant Physiol.*, *101*, 37–47.

Harrison, S. P., and I. C. Prentice (2003), Climate and CO_2 controls on global vegetation distribution at the last glacial maximum: Analysis based on palaeovegetation data, biome modelling and palaeoclimate simulations, *Global Change Biol.*, *9*, 983–1004.

Harzallah, A., and R. Sadourny (1995), Internal versus SST-forced atmospheric variability as simulated by atmospheric general circulation model, *J. Clim.*, *8*, 474–495.

Haxeltine, A., and I. C. Prentice (1996), BIOME3: An equilibrium terrestrial biosphere model based on ecophysiological constraints, resource availability, and competition among plant functional types, *Global Biogeochem. Cycles*, *10*(4), 693–709.

Helman, Y., E. Barkan, D. Eisenstadt, B. Luz, and A. Kaplan (2005), Fractionation of the three stable oxygen isotopes by oxygen producing and consuming reactions in photosynthetic organisms, *Plant Physiol.*, *138*, 2292–2298.

Hoffmann, G., M. Werner, and M. Heimann (1998), The water isotope module of the ECHAM atmospheric general circulation model: A study on timescales from days to several years, *J. Geophys. Res.*, *103*, 16,871–16,896.

Hoffmann, G., et al. (2004), A model of the Earth's Dole effect, *Global Biogeochem. Cycles*, *18*, GB1008, doi:10.1029/2003GB002059.

Jouzel, J., G. Hoffmann, R. D. Koster, and V. Masson (2000), Water isotopes in precipitation: Data/model comparison for present-day and past climates, *Quat. Sci. Rev.*, *19*, 363–379.

Kaduk, J., and M. Heimann (1996), Assessing the climate sensitivity of the global terrestrial carbon cycle model SILVAN, *Phys. Chem. Earth*, *21*(5–6), 529–535.

Kohfeld, K. E., C. Le Quere, S. P. Harrison, and R. F. Anderson (2005), Role of marine biology in glacial-interglacial CO_2 cycles, *Science*, *308*, 74–78.

Krinner, G., N. Viovy, N. de Noblet-Ducoudré, J. Ogée, J. Polcher, P. Friedlingstein, P. Ciais, S. Sitch, and I. C. Prentice (2005), A dynamic global vegetation model for studies of the coupled atmosphere-biosphere system, *Global Biogeochem. Cycles*, *19*, GB1015, doi:10.1029/2003GB002199.

Landais, A., E. Barkan, D. Yakir, and B. Luz (2006), The triple isotopic composition of oxygen in leaf water, *Geochim. Cosmochim. Acta*, *70*, 4105–4115.

Lathiere, J. (2005), Evolution des émissions de composés organiques et azotés par la biosphère continentale dans le modèle LMDz-INCA-ORCHIDEE, doctorate thesis, Univ. of Pierre and Marie Curie, Paris.

Lloyd, J., and G. D. Farquhar (1994), ^{13}C discrimination during CO_2 assimilation by the terrestrial biosphere, *Oecologia*, *99*, 201–215.

Loveland, T. R., B. C. Reed, J. F. Brown, D. O. Ohlen, J. Zhu, L. Yang, and J. W. Merchant (2000), Development of a global land cover characteristics database and IGBP DISCover from 1-km AVHRR Data., *Int. J. Remote Sens.*, *21*(6–7), 1303–1330.

Luz, B., and E. Barkan (2000), Assessment of oceanic productivity with the triple-isotope composition of dissolved oxygen, *Science*, *288*, 2028–2031.

Luz, B., and E. Barkan (2005), The isotopic ratios O-17/O-16 and O-18/O-16 in molecular oxygen and their significance in biogeochemistry, *Geochim. Cosmochim. Acta*, *69*(5), 1099–1110.

Luz, B., E. Barkan, M. L. Bender, M. H. Thiemens, and K. A. Boering (1999), Triple-isotopic composition of atmospheric oxygen as a tracer of biosphere productivity, *Nature*, *400*, 547–550.

Malaizé, B., D. Paillard, J. Jouzel, and D. Raynaud (1999), The Dole effect over the last two glacial-interglacial cycles, *J. Geophys. Res.*, *104*, 14,199–14,208.

Meijer, H. A. J., and W. J. Li (1998), The use of electrolysis for accurate $\delta^{17}O$ and $\delta^{18}O$ isotope measurements in water, *Isotopes Environ. Health Stud.*, *34*, 349–369.

Miller, M. F. (2002), Isotopic fractionation and the quantification of ^{17}O anomalies in the oxygen three-isotopes system: An appraisal and geochemical significance, *Geochim. Cosmochim. Acta*, *66*(11), 1881–1889.

Mora, G., and L. M. Pratt (2001), Isotopic evidence for cooler and drier conditions in the tropical Andes during the last glacial stage, *Geology*, *29*, 519–522.

Navarro, N., C. Lecuyer, S. Montuire, C. Langlois, and F. Martineau (2004), Oxygen isotope compositions of phosphate from arvicoline teeth and Quaternary climatic changes, Gigny, French Jura, *Quat. Res.*, *62*, 172–182.

Poutou, E., G. Krinner, C. Genthon, and N. de Noblet-Ducoudré (2004), Role of soil freezing in future boreal climate change, *Clim. Dyn.*, *23*, 621–636.

Ramankutty, N., and J. A. Foley (1999), Estimating historical changes in global land cover: Croplands from 1700 to 1992, *Global Biogeochem. Cycles*, *13*(4), 997–1027.

Ray, N., and J. M. Adams (2001), A GIS-based vegetation map of the world at the Last Glacial Maximum (25,000–15,000 BP), *Internet Archaeol.*, *11*, http://intarch.ac.uk/journal/issue11/rayadams_index.html.

Ribas-Carbo, M., S. A. Robinson, M. A. Gonzalez-Meler, A. M. Lennon, L. Giles, and J. A. Berry (2000), Effects of light on respiration and oxygen isotope fractionation in soybean cotyledons, *Plant Cell Environ.*, *23*(9), 983–989.

Schlesinger, W. H., and J. A. Andrews (2000), Soil respiration and the global carbon cycle, *Biogeochemistry*, *48*, 7–20.

Thiemens, M. H., T. Jackson, K. Mauersberger, B. Schueler, and J. Morton (1991), Oxygen isotope fractionation in stratospheric CO_2, *Geophys. Res. Lett.*, *18*, 669–672.

von Caemmerer, S. (2000), *Biochemical Models of Leaf Photosynthesis*, *Tech. Plant Sci. Ser.*, vol. 2, Commonw. Sci. and Ind. Res. Org., Collingwood, Victoria, Australia.

von Grafenstein, U., H. Erlenkeuser, A. Brauer, J. Jouzel, and S. Johnsen (1999), A mid-European decadal isotope-climate record from 15,500 to 5000 years BP, *Science*, *284*, 1654–1657.

Waelbroeck, C., L. Labeyrie, E. Michel, J.-C. Duplessy, J. F. McManus, K. Lambeck, E. Balbon, and M. Labracherie (2002), Sea level and deep temperature changes derived from benthic foraminifera benthic records, *Quat. Sci. Rev.*, *21*, 295–306.

E. Barkan, A. Landais, and B. Luz, Institute of Earth Sciences, Edmond Safra Campus, Hebrew University of Jerusalem, Givat Ram, 91904 Jerusalem, Israel. (landais@vms.huji.ac.il)

J. Lathiere, IPSL/LSCE, CNRS/CEA, F-91191 Gif sur Yvette, France.